Statistical Analysis of Eddy Current NDT related to Aircraft Structures

By

Omer Zia Siddiqui

2013-NUST-MS Electrical (Communication)-NUST201362888MPNEC45313F

Supervised by

Captain Dr. Tariq Mairaj Rasool Khan PN

A dissertation submitted to

PAKISTAN NAVY ENGINEERING COLLEGE
NATIONAL UNIVERSITY OF SCIENCES AND TECHNOLOGY, ISLAMABAD

in partial fulfillment of the requirements for the degree of

MS ELECTRICAL ENGINEERING (COMMUNICATIONS)

July 2017

Thesis Title:

Statistical Analysis of Eddy Current NDT related to Aircraft Structures

Thesis submitted in partial fulfillment of the requirements for the degree of Master of Science in Electrical Engineering with specialization in Communications to the Department of Electronics and Power Engineering at PNEC-NUST.

Submitted by:

Omer Zia Siddiqui
Reg. No.NUST201362888MPNEC45313F

Supervised by:

Captain Dr. Tariq Mairaj Rasool Khan PN
Assistant Professor
Department of Electronics and Power Engineering

Guidance and Examination Committee:

1. Cdr. Dr. Adeel Yousuf — Assistant Professor (EPE)
2. Cdr. Dr. Aleem Mushtaq — Assistant Professor (EPE)

Approval Page

TH-4 page (signed and approved) will come in-place of this page.

Table of Contents

List of Figures

List of Tables

List of Abbreviations

NDT	Non-Destructive Testing
NDE	Non-Destructing Evaluation
EC	Eddy Current
UT	Ultrasonic Testing
EC NDT	Eddy Current Non Destructive Testing
CBM	Condition Bed Monitoring
RCM	Reliability Centered Maintenance
SQP	Sequential Quadratic Programming

Abstract

Flaw profile characterization from non-destructive evaluation (NDE) measurements is a typical NDT inverse problem. Importance of flaw profiling particularly in aerospace industry is paramount as it is a decision tool to evaluate air worthiness of the aero-structures. Accurate flaw profiling thus ensures aircraft safety through implementation of cost effective replacement/repair schemes.

Eddy current (EC) data acquired at multiple frequencies contain complementary information about flaws due to skin effect phenomenon. However, finding the exact contribution of each flaw under the EC scan area in generation of resultant EC measurement and effect of each measurement mode (scan frequency) while determining the solution to inverse problem is considerably challenging. In the reported research work, statistical analysis of flaw profile and corresponding multimode EC measurements has been undertaken both as a forward problem and inverse problem. Forward relation analysis between flaw profile and EC measurements assisted to find the effect/contribution of the flaws, spread around a central scan point on a specimen under test, in generating EC measurements,. Whereas, inverse relation analysis assisted in formulation of a novel multi-frequency eddy current data based polynomial model to solve the inverse problem for re-construction of flaw profile.

Chapter 1 Introduction

1.1 Background and motivation

Aircraft safety is primarily dependent on its structural health. For safe operations of the aircraft whether it be a passenger liner or a military one, it is essential to keep an eye on the structural state of the plane. Periodic maintenance require down time of the aircraft and also involve money for replacement of parts and associated maintenance work. Though this on one hand ensures safety; however, on the other hand it effects the operational availability of the platform. This is neither feasible for passenger liners looking for high rate of passenger transportation to generate finance and profit; Likewise same is not appreciated by military organizations due lowered asset availability and overall readiness. In order to address the problem and to maximize operational availability with safety assurance, researches were undertaken result in the concept of Reliability Centered Maintenance (RCM). RCM is based on Condition Based Monitoring (CBM) to effectively monitor specimen status particularly when a potential failure symptoms have been observed. EC Non Destructive Evaluation (EC NDE) is one of the popular and historic technique to evaluate the health status of aircraft structure.

Various forward models are available to estimate the eddy current measurements being generated from the structure. But of course there is always a gap

between the theoretical model and the practical minutes. Hence there is a requirement to bridge the gap and carry out statistical analysis with an aim to provide more fitting models for flaw profiling of the structures under test. In particular the research analysis is focused on aircraft structure having prime importance in both civil as well as military use.

Likewise Inverse relation modeling is also essential and commonly applied to reconstruct the flaw profile from the available measurements data. The topic of research has been an area of interest since long and is still an active research domain being directly related to safety of men & material in both civil and military aviation industries.

Chapter 2 Literature Review

The phenomenon of eddy currents was discovered by French physicist Leon Foucault in 1851, and for this reason eddy currents are sometimes called Foucault currents. Foucault built a device that used a copper disk moving in a strong magnetic field to show that eddy currents (magnetic fields) are generated when a material moves within an applied magnetic field.

Aviation industry cannot afford 'Run to fail' or 'Fix when fail' concepts due extremely high safety consideration associated due obvious reasons. At the same time minimization of down time of the platforms is essential to make the operations safe and cost effective. This required informed decision making based on certain evaluations and judgments. Though air accidents have reduced with improvement in technology and testing techniques, however the probability of accidents still exists. A Boeing 707 crashed in 1977 after 16,723 flights because it lost a horizontal tail plane due to a fatigue failure in a spar [1]. According to a review of U.S. Air Force, most structure failures initiates as surface cracks or cracks at rivet-holes [2]. In order to undertake informed decisions, EC NDT is often used for aircraft structural health monitoring.

Various Aerospace defects are illustrated in Figure 1-1.

`

Fig 1-1 Common Aerospace defects

2.1 Eddy Current Non-Destructive Testing (EC NDT)

Eddy current inspection is one of several NDT methods that use the principle of electromagnetism as the basis for conducting examinations. Eddy currents are created by electromagnetic induction once alternating current is applied to a scanning coil. Eddy currents normally travel parallel to the coil's winding and their flow is limited to the area of the inducing magnetic field. Density of the eddy currents is more near the surface adjacent to an excitation coil; whereas concentration decreases with distance from the coil, exponentially with depth. This phenomenon is known as the skin effect.

Skin effect reflects the ability of test signal to penetrate in the specimen. Skin depth can be calculated by equation (1), as a well-established fact.

$$\delta = 1/\sqrt{\sigma \mu_0 \mu_r f} \qquad (1)$$

Where, δ is standard penetration depth (mm), σ is material electric conductivity, μ_0 is absolute permeability, $\mu_r$is relative permeability and f is frequency of the EC signal.

It can be noted that skin depth is inversely proportional to square root of all the parameters of the equation (1). It is also evident from the above equation that materials having poor or relatively low permeability, do not qualify to undergo an eddy current NDT.

From equation (I), effects of the frequency of the signal being used, can be deduced. Lower is the frequency, more is the penetration depth and vice versa. Therefore, to have better flaw depth information, low frequencies are more suitable. However, they have handicap in terms of surface resolution - a measure of how closely lines/flaws can be resolved in an image.

From above discussions, it can be deduced that multi frequencies carry complementary information pertaining to flaws. This gives rise to the requirement of data fusion of the multi-mode EC data.

Flaw profiling using eddy current multi modal measurements has been an area of interest of researchers. Flaw profiling of structures using NDE is a typical inverse problem, which is ill posed due non-uniqueness [3]. Profiling of cracks or flaw growth as a function of spatial position becomes more challenging in the presence of

measurement noise. Various techniques have been proposed in the literature to address the ill-posedness [3]

As discussed Eddy current (EC) data acquired at multiple frequencies contain complementary information about flaws. Accordingly, many researchers have employed data fusion techniques to solve the NDE inverse problem [4], [5]. Commonly proposed solutions include neural networks [6]– [7], Bayesian analysis based on the Dempster–Shafer evidence theory [8]– [9], wavelet and other multi resolution algorithms [7], and image fusion [10], [11] [12], in the time and-frequency domain. These methods have been applied to fuse NDE data from a range of sources, including multi frequency eddy current testing (ECT) [5] [6], [13]; ECT data and ultrasound measurements [6], [13], [11], [12]; ultra sound, X-ray, and acoustic emission measurements [9]; and other techniques (such as pulsed eddy current measurements) [14]. In addition to these fusion techniques, other methods such as a Q-transform-based technique [15] were also investigated earlier.

It is quite challenging for the researchers to model and formulate the real occurring phenomena in totality. Therefore many statistical approaches were proposed to deal with this type of processes.

2.2 Statistical Analysis

Statistical analysis is the numerical approach to analyze two or more interdependent data sets. Typically, a few of them forms the independent set of

variables and others dependent ones. The data is assumed to embed all physics of underlying processes. Accordingly while doing statistical analysis, physical effects of parameters are not taken into account separately and it is considered that data being analyzed caters all applicable effects, relations, co-relations. It is also assumed that the observation(s) /measurement(s) is the net cumulative outcome, which is comparatively easier to handle through statistical analysis, for complex processes, particularly. The focus of this research is also statistical evaluation of EC NDT w.r.t the Flaw profile with particular focus on the effect of spatial neighborhood on the measurements.

Chapter 3 Case Study

3.1 Problem Formulation

A 30 years old retired Boeing aircraft fuselage structure was used as the case study. Two specimens (C and D) from the Boeing 727 aircraft, are shown in Fig. 3-1. The thickness of each layer of aluminum 2024-T3 lap joint is 0.045 in (1.143 mm). True profile was extracted from X-ray data, whereas actually acquired multiple frequency (5.5, 8, 17 and 30 kHz) EC data from the structure was used as measurement data. The flaw profile and the measurement data form mutually exclusive training (specimen/section C) and test (specimen/section D) data sets.

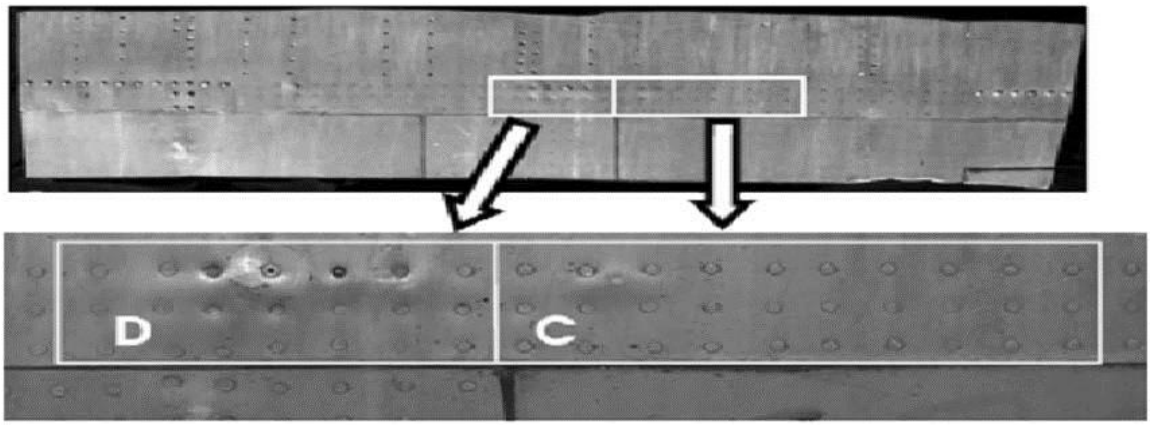

Fig 3-1 Aircraft fuselage specimens (C and D)

The flaw profile and the multimode EC NDE measurement data used as training set as well as dependent and independent variables data sets are shown in Fig-32,

where X-Ray data serves as independent variable or Truth profile and EC measurements are taken as dependent variable data set.

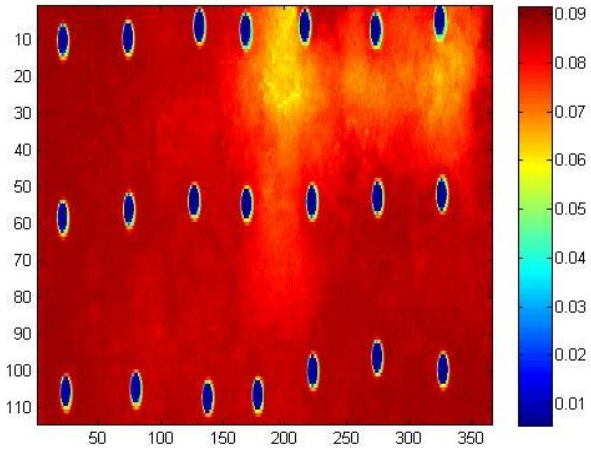

(a) Flaw Profile (X-Ray Image)

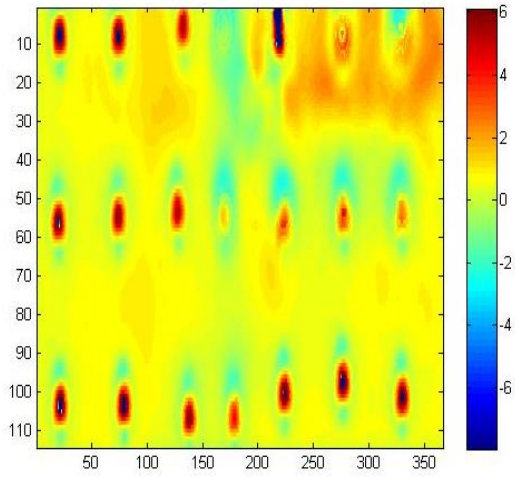

(b) EC Measurements at 17 kHz

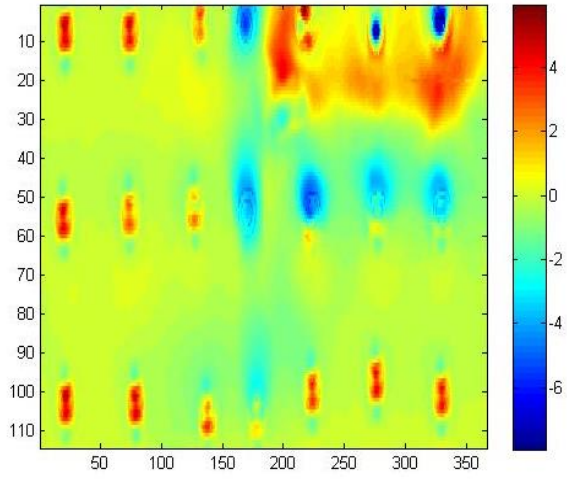

(c) EC Measurements at 17 kHz

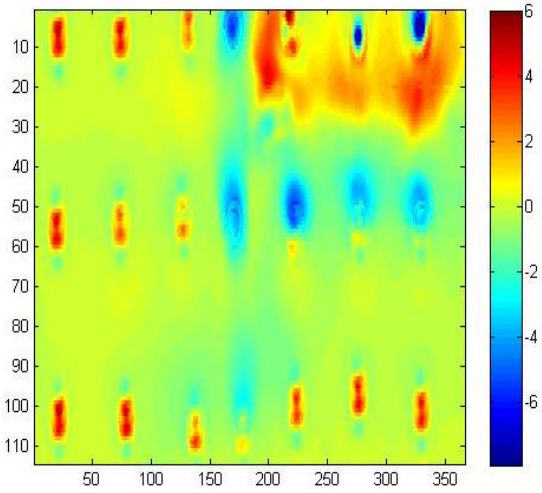

(d) EC Measurements at 30 kHz

Figure 3-2 (a) The flaw profile (X-Ray image) and Figure 3-2 (b) to (d) - Measurements at each frequency mode of Section C of Aircraft Fuselage

Data and measurements are zero mean arranged. Both X-ray data and eddy current measurements are arranged in matrix of size 114 x 366 both corresponding to

identical spatial point. The statistical parameters of the X ray data (or flaws profile) and EC measurements are tabulated below in Table-3-I:

TABLE 3-I STATISTICAL PARAMETERS OF FLAW PROFILE AND MULTI FREQUENCY EC MEASUREMENTS

Parameters	Flaw Profile (X-Ray Data)	Measurements		
		8 kHz	17 kHz	30 kHz
Mean	0.08	0.562	-0.228	-0.228
Std Deviation	0.013	1.009	1.127	1.145
Variance	1.89e-04	1.018	1.270	1.311
Min Value	0.005	-7.963	-7.934	-7.929
Max Value	0.091	6.118	5.967	6.020
# of Unique Values	41656	1542	1891	1935

As obvious from the table, the dynamic range of profile is less as compared to the EC measurements values, indicating high sensitivity of Eddy Current (EC) NDT methodology. Non-uniqueness is also evident, as highlighted by the difference in the number of unique values of profile and the EC measurements. The above mentioned observations indicate usefulness of application of inverse EC modeling in flaw profile computation, which can address the ill-posedness of EC NDT data. Therefore, the research pertaining to accurate inverse modeling in addition to statistical analysis of forward relation between truth profile and the measurements contains value.

Chapter 4 Methodology - Forward Case

During analysis of forward relation between truth profile and measurements (Ref to Table-3-1), it was noted that dynamic range (i.e. difference between minimum and maximum values) of measurements or EC NDT data is quite large as compared to truth profile or X-Ray data. This indicate high sensitivity of EC NDT technique and shows ability of EC NDT response even with a little change in flaw profile. This supports the efficacy and usefulness of using EC NDT technique.

It was also observed that number of unique values of Truth profile (X-Ray data) is quite high as compared to number of unique values of Multimode Measurement data. As tabulated in Table 3-1, number of unique values of Truth profile is 41656 and that of measurements is from 1500 to 2000 for multimode measurements data from 8 kHz to 30 kHz. This indicates the ill-posedness of the problem. However, forward relation is much more ill-posed as compared to inverse problem. This is also noteworthy that this ill posedness is when we relate truth profile and measurements point to point.

For the purpose of analysis X-ray data was binned in 9 bins as per spread of the data and plotted against Eddy Current values at a particular measurement (frequency) mode as given in Fig 4-1. Non uniqueness problem is quite evident as a number of EC measurement values can be noted in the plot against unique X-ray data value.

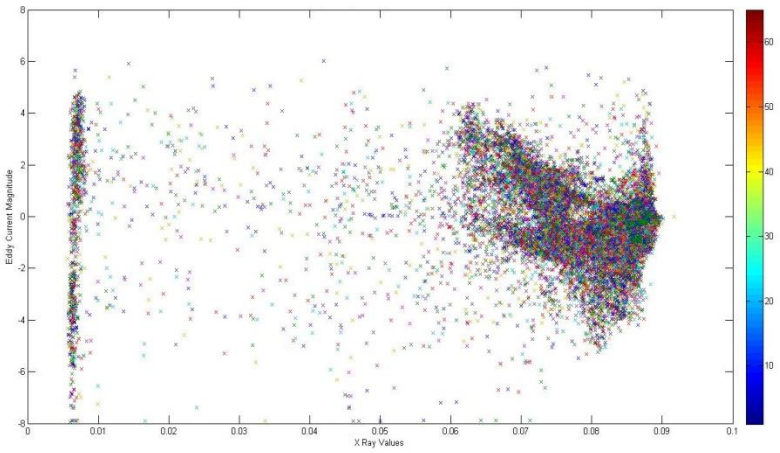

Figure 4-1 X-Ray Vs Eddy Current Values

4.1 Foot Print of the EC Probe

Footprint of the probe was tried to be evaluated statistically by evaluating the effect of a distant X-ray profile change. It can be realized that the scanning EC probe has a certain diameter/cross section area generating Eddy Current in the specimen. Therefore, it was necessary to establish the portion which of truth profile which is cumulatively generating measurements, when EC probe is placed at a particular point. Among the available measurements and truth profile data sets, an area was located where there was no change in flaw depths till certain distance. Response changes in measurements were observed statistically and it was found that measurements start changing approximately before the crack is reached by the EC probe center point. The discussion can be better understood by the Figure 4-2 given below:

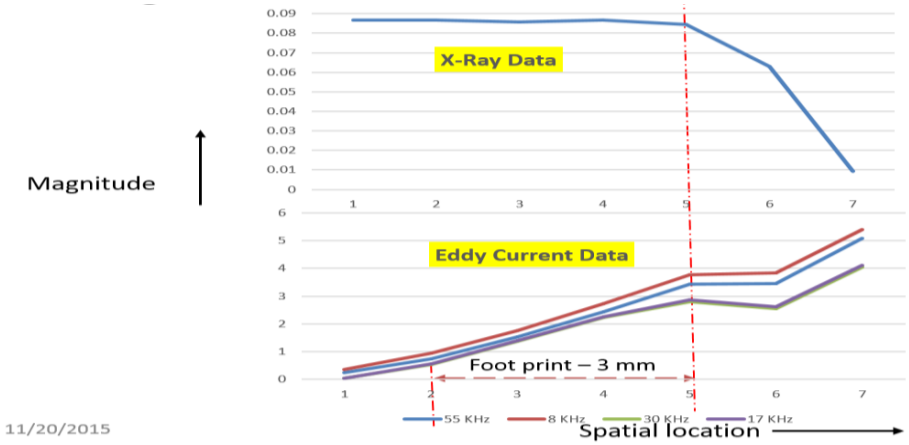

Figure 4-2 Evaluating EC Probe Footprint

Based on the foot print observed, it was decided to evaluate a 3 x 3 matrix of truth profile with center point at X(r,c) – this block of X-ray data as shown in Fig 4-3 was assumed to be generating the measurements and remained the focus of research as far as analysis of effects of neighbor is concerned. X-Ray data spread from Min value of 0.005 to a max of 0.091 is divided into 9 bins for analysis.

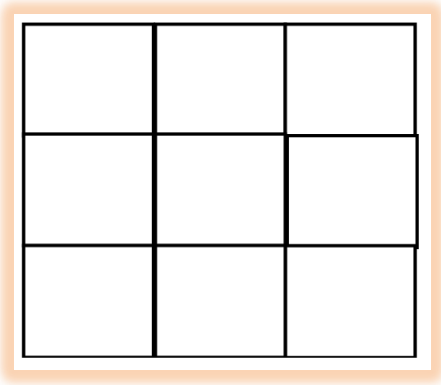

Figure 4-3 3 x 3 Matrix of Truth Profile

As one of the objective of the research work, contribution of neighborhood flaws in generating the measurements was studied statistically. It was considered that though weights of the neighborhoods can be calculated by regression analysis, however major

drawback was that the co-efficient of each neighborhood would be fixed – same is actually not the case as flaws can vary at any neighborhood location and accordingly its weight or co-efficient has to be variable. Due to this consideration, a dynamic weight allocation to neighbor was studied.

In order to evaluate weights of the neighbors for subsequent incorporation in the model development, Effects of neighbors attempted to be quantified using equal weight contribution and half weight contributions of 8 x neighboring values. Equations used to combine the truth profile values at the point under test (say location/point r,c) are as given below.

For Equal Wts

L(r,c) = 0.1111*(xrayC(r,c) + xrayC(r-1,c) + xrayC(r+1,c) + xrayC(r,c-1) + xrayC(r-1,c-1) +xrayC(r+1,c-1) + xrayC(r,c+1) + xrayC(r-1,c+1) + xrayC(r+1,c+1));

For Half Wts

L(r,c) = 0.5*xrayC(r,c) + 0.0625*(xrayC(r-1,c) + xrayC(r+1,c) + xrayC(r,c-1) + xrayC(r-1,c-1) + xrayC(r+1,c-1) + xrayC(r,c+1) + xrayC(r-1,c+1) + xrayC(r+1,c+1));

Error bars at different Frequencies are shown in Fig 4-4. Y axis denote error bar plot of EC measurements mean value taken in each bin of truth profile. The figure shows EC error bars in each measurement mode against X-ray data bins. Furthermore, three

plots in each EC measurement mode pertains to the case when all data points (centre point and neighborhood) were allocated either no weight or equal or half weights. Results were not conclusive and only thing drawn out of it was that we have comparatively less error bar plot for the cases where flaws are less.

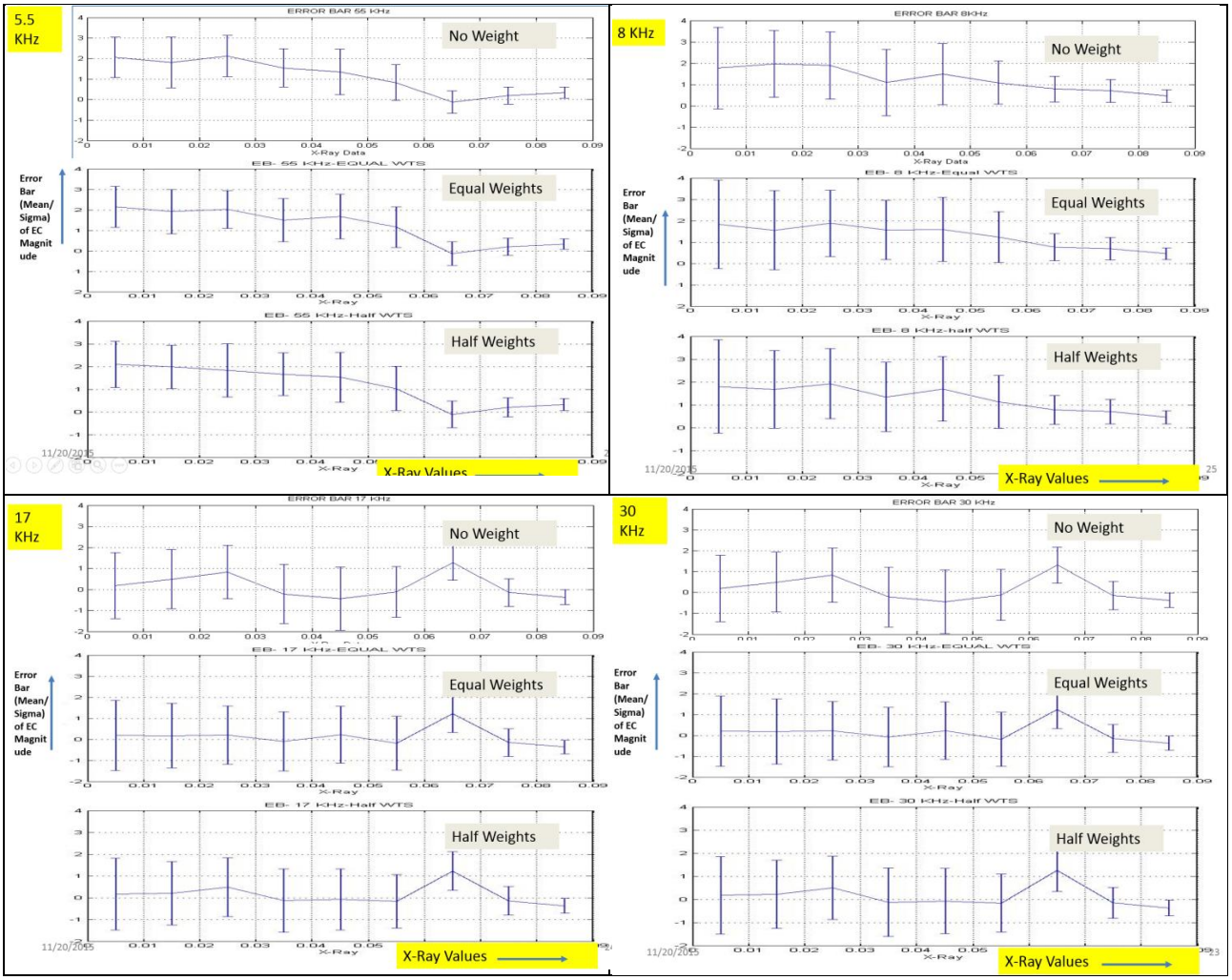

Figure 4-4 Error Bar Plot of EC Measurement Modes

Spread of EC measurements were also modeled by curve fitting and plotted in Figures 4-5 and 4-6. Histogram appearing in the picture indicates the truth profile data whereas Gaussian curves are the EC measurements in each frequency mode. The

results also indicated the ill posedness; however variance of the Gaussian plots can be seen of lesser values at low frequencies of 5.5 and 8 kHz as compared to 17 and 30 kHz.

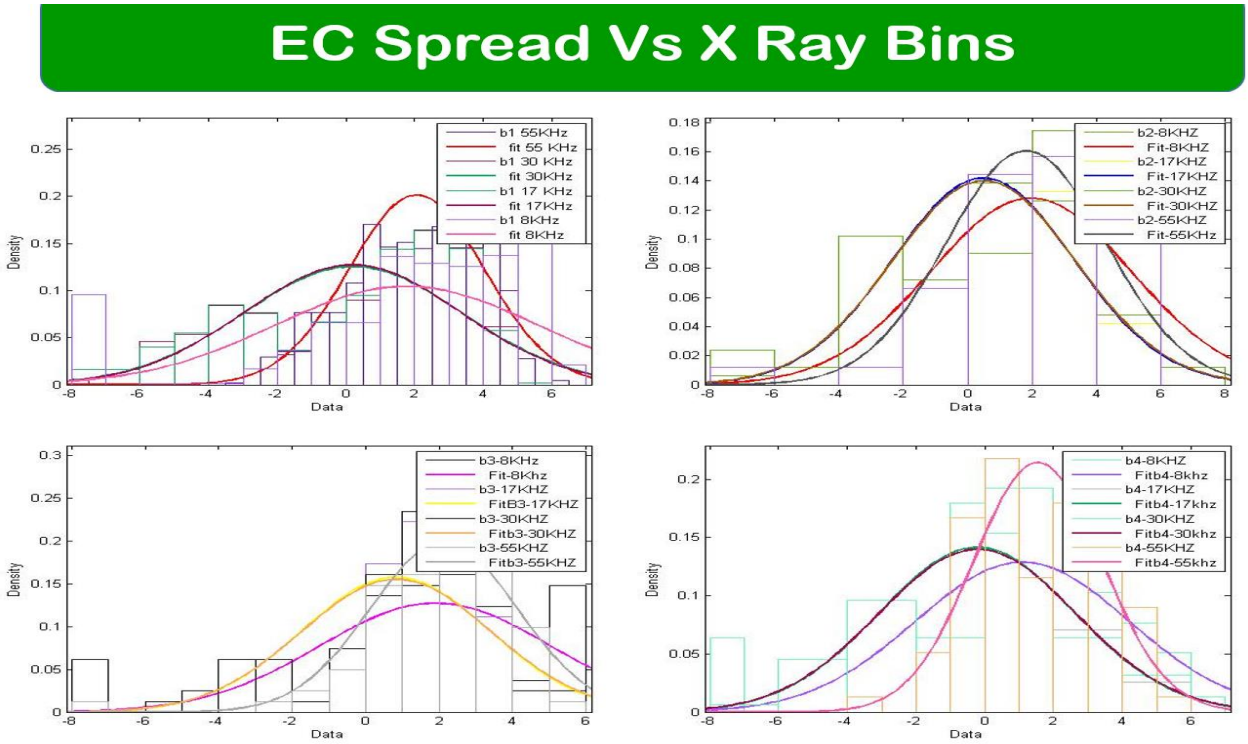

Figure 4-5 EC spread Vs Xray Bins 1 to 4

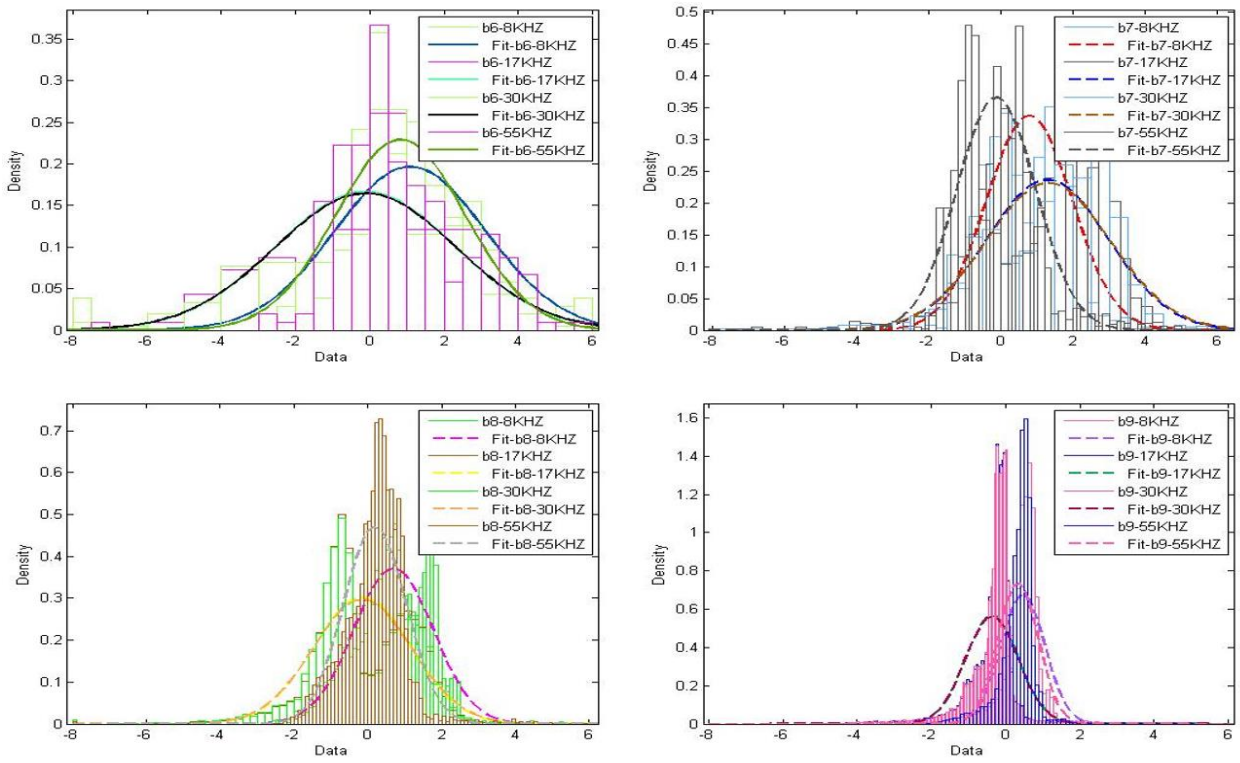

Figure 4-6 EC spread Vs Xray Bins 5 to 9

As another way of statistical analysis, percentage error i.e. ratio of standard deviation and mean value of EC measurements in a particular bin were plotted to calculate percentage error. For the same EC measurements values against X-ray bin value were identified. Subsequently Mean and standard deviation were then calculated and plotted as percentage error graph for each X-Ray bin data. It was pertinently observed that percentage error reduces significantly where flaws are less i.e towards X-Ray bins 6 and above. It was also noted that low frequencies (5.5 and 8 kHz) have less %error in areas where flaws depths are higher. This is probably due to reason that low frequencies can penetrate more into specimen under test as compared to higher frequencies. Percentage error graph is ploted in Fig 4-7 and tabulated in Table 4-I – X

axis shows truth profile bins (first bin having highest flaw depths and also holes in rivet areas whereas bins towards right have less flaw depths or we can say lesser eroded areas of aircraft fuselage). Y-axis indicate the % error calculated as ratio of standard deviation and mean of EC measurements corresponding to that X-Ray bin.

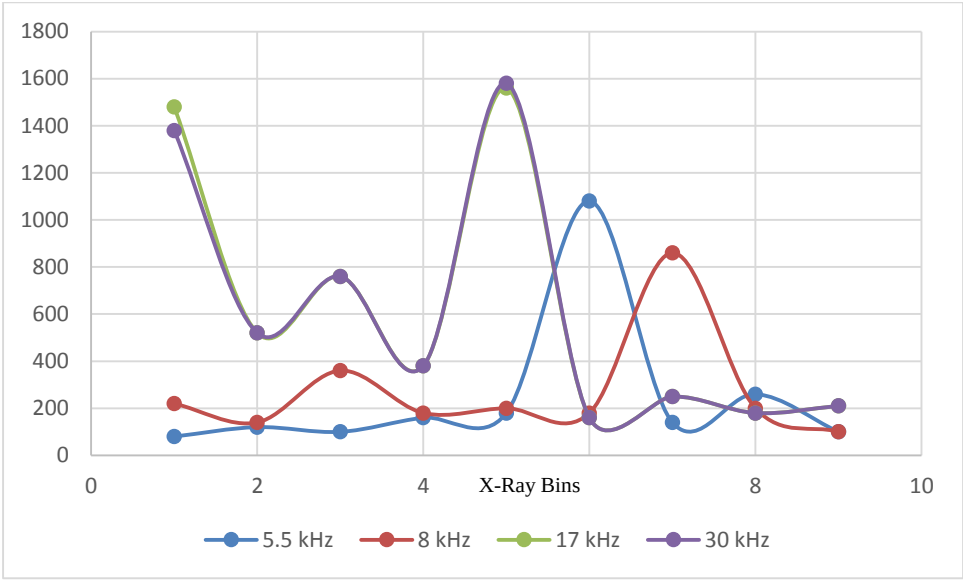

Figure 4-7 Percentage Error – X-Ray Bins Vs Frequencies

TABLE 4—1 Percentage Error – X-Ray Bins Vs Frequencies

X-Ray Bins	Frequency (kHz)			
	5.5	8	17	30
1	80	220	1480	1380
2	120	140	520	520
3	100	360	760	760
4	160	180	380	380
5	180	200	1560	1580
6	1080	180	160	160
7	140	860	250	250
8	260	200	180	180
9	100	100	210	210

What can we deduce at this point, is that correlating truth profile and measurements point by point values is not the right approach, particularly in forward problem modeling. This can be visualized that by this analysis/modeling approach, we are actually relating data/measurements physically present at different locations without considering the adjacent/neighboring structure/flaws.

In further study/analysis, the approach adopted included: Polynomial modeling of various orders/degrees were undertaken, then the effects of neighborhood profile of 3 x 3 matrix area as illustrated in Fig 4-3 was evaluated by various statistical parameters. During research it was noted that physics of the problem is such that fixed weights cannot be assigned to the neighboring locations – even optimization through regression may not capture the physical model closely. Based on this it was appreciated that the neighborhood effect should not be static fixed values rather they should be considered as dynamic contributors for the area under eddy current scan at any given time/location as the flaw can occur or grow at any spatial position near center point X(r,c).

The method to evaluate neighboring effect was as under:

a. The measurements (response) were approximated from the state through an Nth order polynomial based model as given in equation (2), based on the results reported in [3].

$$z_k = \sum_{n=0}^{N} c_n x_k^{\,n} \qquad (2)$$

b. Model was used to construct/imitate the multi-mode EC measurements by putting the values of Truth profile x_k in the following manner:

(1) Value of x_k was taken as X(r,c) point value.

(2) Value of x_k was taken as Max [A] considering the foot print block shown at Fig 4-3

(3) Value of x_k was taken as Mode [A].

(4) Value of x_k was taken as Mean [A].

Where A = {X(r,c), X(r,c-1), X(r,c+1), X(r-1,c), X(r-1,c-1), X(r-1,c+1), X(r+1,c), X(r+1,c-1),X(r+1,c+1)}

The constructed multi-mode EC profiles were compared with actually observed measurements using a quantitative metric known as Mean Square Error (MSE), as given in equation (5) to ascertain effects of various statistical parameters application:

$$MSE = \sqrt{\sum (P - \hat{P})^2} / XY \qquad (5)$$

Where P is the true profile and $\hat{P}$ is the computed profile.

It was noted that lower frequencies of 5.5 and 8 kHz showed better response in terms of MSE if we consider Max or Mode of the scan area for forward profile development. On the other hand effect of higher frequencies of 17 and 30 kHz were almost same on all modes with slight better MSE values when we apply Mean value of the scan area for forward profile construction.

Results are illustrated in Fig 4-8 and tabulated in Table 4-2.

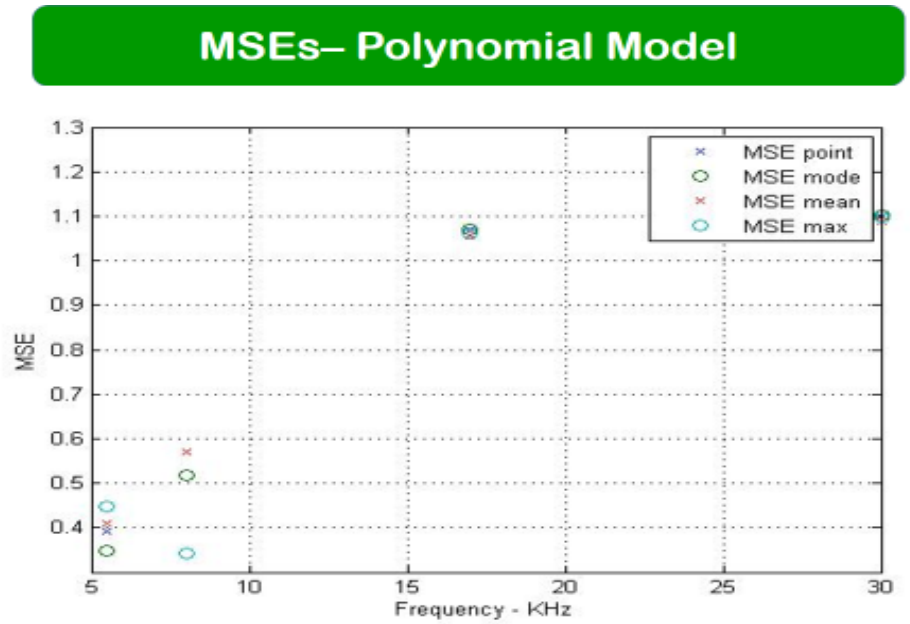

Figure 4-8 FORWARD EC PROFILE RE-CONSTRUCTION WITH VARYING STATISTICAL PARAMETERS

TABLE 4-2 RESULTS IN TERMS OF MSE – FORWARD EC PROFILE RE-CONSTRUCTION WITH VARYING STATISTICAL PARAMETERS

Frequency (kHz)	MSE			
	MSE POINT	MSE MODE	MSE MEAN	MSE MAX
5.5	0.39	0.3	0.41	0.45
8	0.58	0.52	0.58	0.29
17	1.08	1.08	1.06	1.08
30	1.09	1.1	1.09	1.1

4.2 Statistical Analysis Deductions – General and Forward Case

Following can be deduced from the analysis presented in this chapter up till now:

a. Eddy Currents Measurements are quite sensitive to changes in Truth Profile. For a change of flaw depth from 0.005 to 0.091 only change in measurements is approximately from -7.9 to 6.2

b. Number of unique values of Truth profile (X-Ray data) is quite high as compared to number of unique values of Multimode Measurement data, indicating ill posedness of the problem.

c. EC measurements modeling against specific bin value of X-ray data gave significant Error bar values or variance around mean value, indicating significance to consider neighbor profile effect in EC measurement generation.

d. Percentage error (ratio of standard deviation and mean) is comparatively less for low frequencies as compared to higher frequencies, where flaw depth is more indicating penetration ability of EC signal in the specimen under test.

e. Physics of the EC NDT can be modeled better considering the effect of neighboring flaw profile effects as a dynamic case instead of assigning fixed weights/co-efficient to specific spatial neighbor.

f. Low frequency of 8 kHz measurements when re-constructed using max value of scan area were low in terms of MSE. On the other hand, effect of higher frequencies of 17 and 30 kHz were slightly better w.r.t MSE values when re-constructed using Mean value of the scan area for forward profile construction.

Chapter 5 Statistical Analysis - Inverse Case

During the case study usefulness was noted of application of inverse EC modeling in flaw profile computation, which can address the ill-posed ness of EC NDT data. Therefore the research in addition to statistical analysis of forward relation between truth profile and the measurements was also motivated to the application of inverse EC multi-mode modeling for flaw profiling.

5.1 Curve Fitting - Single Frequency Mode Data Modeling.

Curve fitting relates one or more dependent variables to the independent variable, with a certain confidence level. However, for ill posed problems, curve fitting is complex and require statistical analysis for selection of the appropriate model based on the goodness of fit parameters. Polynomial curve fitting finds the coefficients of a polynomial p(x) of degree, 'n' that fit the data, p(x(i)) to y(i), in a least squares sense, where 'i' is the running index indicating spatial location of data x and corresponding measurement y.

A comparative study using different measurement models to establish relationship between the flaw profile and low-frequency electromagnetic NDE measurements, in terms of inversion accuracy and computational load, was undertaken. The measurements (response) can be approximated from the state through an Nth order polynomial based model as given in equation (1), based on the results reported in [16].

$$z_k = \sum_{n=0}^{N} c_n x_k{}^n \qquad (1)$$

Where x_k is flaw profile or True (X-Ray) data at spatial location k, z_k is Eddy Current measurement magnitude at location k at given frequency and c_n is co-efficient associated to the degree of polynomial.

However, the proposed approach to solve the EC inverse problem is to approximate the inverse given in (2) from the empirical data. Then the model, so acquired, is applied on EC measurement data to compute the flaw profile.

$$x_k = \sum_{n=0}^{N} c_n z_k{}^n \qquad (2)$$

Parameters of equation (2) are same as already defined above. The approach eliminated the likely calculation in-accuracies which might be experienced during inversion of a forward relationship. Polynomials of varying degrees were fitted on the training data corresponding to each scan frequency to finalize the optimum degree of polynomial for each frequency.

5.2 Inverse Model Optimization

As the output of the inverse model flaw profile, is dependent upon multiple measurements; appropriate co-efficient/weight assignment to each measurement mode is formulated as a constrained optimization problem. Optimization can be achieved by minimizing the cost function f, given in equation (3):

$$f = norm(|X| - |a_{m1} * Y_{m1} + a_{m2} .* Y_{m2} + a_{m3} .* Y_{m3}|) \qquad (3)$$

Where f is cost minimization function, X is matrix comprising x (i, j) true flaw values such that index i spans from 1 to I and index j spans 1 to J. Y_{m1},Y_{m2}& Y_{m3} are single measurement mode (frequency) reconstructed flaw profile comprising y(i,j) reconstructed flaw values with i= 1 to I and j=1 to J. a_{m1}, a_{m2}, a_{m3} are the weights of the respective measurement modes to be calculated.

The equation offers the difference between the actual flaw profile and the calculated flaw profile using multi-mode ECT data. The cost function can be minimized by assigning optimal weights to the coefficients. The coefficient of each measurement mode can be restricted to range of certain values through introduction of constraints in the proposed framework. The range of values can be specified based on prior information, if any.

5.3 Optimization Techniques.

Constrained non-linear optimization computes minimum of a scalar function under given constraints. The cost minimizing function used is based on a Hessian, which is the second derivative of the Lagrangian. We considered various optimization algorithms to calculate weights of the measurement modes. However, within theoretical boundaries, we considered Sequential Quadratic Programming (SQP) most appropriate [17], being simple and easily applicable to the available test and training data.

5.4 Inverse Eddy Current NDT Modeling for Flaw Profiling

The flaw profile (X-Ray data) and measurements at each frequency mode are given in Figure-1. Equations (2) and (3) were utilized together to finalize measurement models. The polynomial based measurement models of 2nd to 5th order were compared to solve the actual inverse problem through computation of the coefficients of the individual measurement modes. Flaw states can then be computed using available measurements using equation (2). Subsequently fusion is undertaken and weights for each mode are optimized using constrained minimization function at equation (3). The proposed inversion scheme is implemented on the case study discussed in Chapter-3, to showcase the efficacy of the proposed research methodology.

5.5 Implementation and Training of Proposed Multi frequency EC Model Using Training Data

Polynomial models of 2nd to 5th order were used to establish the relationship between the profile and the available EC measurements following equation (3). The effectiveness of curve fitting was measured using a quantitative metric known as Mean Square Error (MSE), as given in equation (4).

$$MSE = \sqrt{\sum (P - \hat{P})^2} \; / \; XY \qquad (4)$$

Where P is the true profile and $\hat{P}$ is the computed profile. MSEs pertaining to measurement data acquired at each scan frequency (8 kHz, 17 kHz and 30 kHz) are tabulated in Table-5-1 and plotted in Figure-5-1.

TABLE 5-1RESULTS - EFFECT OF FREQUENCIES AND POLYNOMIAL ORDER (IN TERMS OF MSE)

Scan Freq	Polynomial Order			
	2nd	3rd	4th	5th
8 kHz	1.23	1.21	1.12	1.12
17 kHz	1.29	1.28	1.26	1.25
30 kHz	1.29	1.28	1.26	1.25

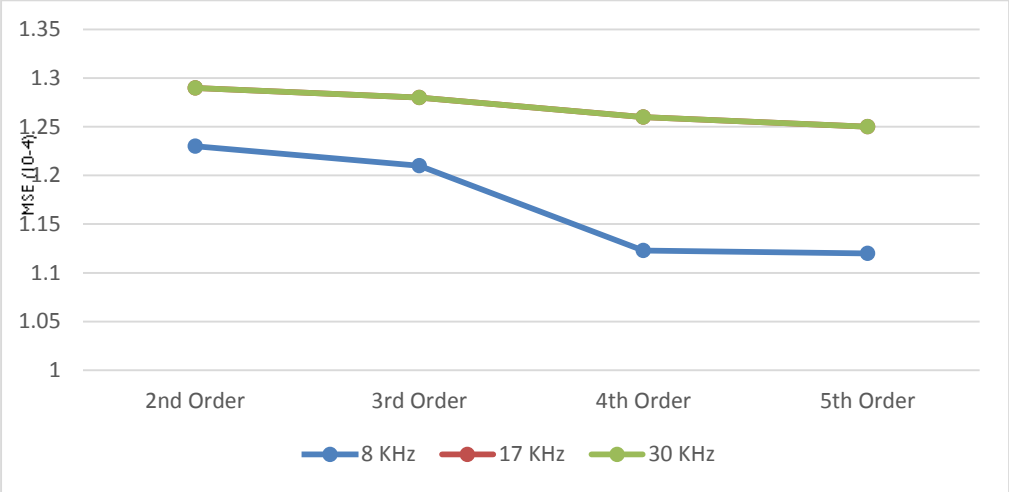

Figure 5-1 Results - Effect of Frequencies and Polynomial Order (In Terms of MSE)

Analysis revealed that higher polynomial models (order 4 & 5) gave better results in terms of MSE as compared to polynomial models 3 and below. Moreover, MSE at lower frequency of 8 kHz was better as compared to 17 & 30 kHz. Above deductions indicate usefulness of higher order polynomial models with comparatively more contribution of low frequency EC measurement mode.

Multi frequencies contain complementary information in terms of flaw depths and surface resolution. Therefore, in order to further refine/optimize the inverse

problem solution for flaw profiling, fusion of the individual frequency models was considered. The curves fitted polynomial models indicate nonlinear relationship between profile and measurements.

As tabulated, MSEs pertaining to low frequency EC measurements are of lesser value, therefore more contribution should be assigned to the lower frequency data in the inverse model which compute profile from multi frequency EC measurements. Based on the above mentioned proportion of curves, a constrained optimization technique was adopted where a-priori knowledge acquired from inversion results using single measurement mode data was used while specifying the constraints of the optimization problem as given in equation (3). Moreover, with the established knowledge of improved results at higher order polynomials, as tabulated in Table-5-1, 4^{th} order was finalized. As above, low frequencies were allocated higher weight ranges (constraint) while optimizing the multi frequency EC fusion based inversion model. The constraints are tabulated in Table-5-2 below:

TABLE-5-2 DATA FUSION OPTIMIZATION – CONSTRAINTS SETTINGS

S No	Constraints
a.	Sum of co-efficient of all EC Measurement modes = 1
b.	Co-efficient range of 8 kHz mode EC data measurement >0.6
c.	Co-efficient range of 17 kHz mode EC data measurement: 0.1-0.3
d.	Co-efficient range of 30 kHz mode EC data measurement: 0.1-0.3
e.	Convergence tolerance limit 10^{-6}

The inversion results using constrained optimization are tabulated in Table-5-3. In order to verify the efficacy of optimized weight scheme, the inversion results (MSEs) were also computed while assigning equal weights to measurements acquired at each

scan frequency. The MSEs obtained using optimized weight scheme and equal weight scheme, with respect to, different measurement models are tabulated in Table-5-3 and plotted in Figure-5-2 for comparison. Results indicate improvement in obtained MSE with multi frequency EC optimized weight fusion based model.

TABLE-5.3 FUSION ANALYSIS - EQUAL WEIGHT TO EACH FREQUENCIES VS CONSTRAINED OPTIMIZATION WEIGHT ASSIGNMENT (IN TERMS OF MSE).

Order	Fused (Equiwt)	Fused (Opt wt)
2nd	1.173	1.12
3rd	1.165	1.11
4th	1.088	1.05
5th	1.075	1.04

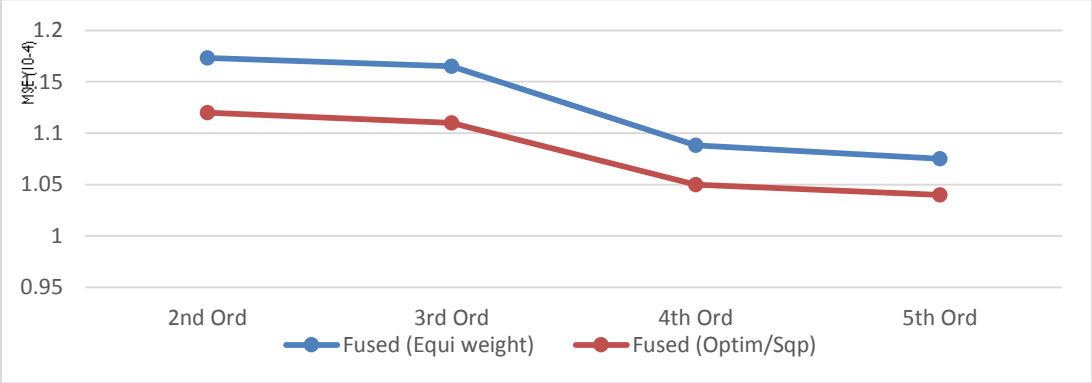

Figure 5-2 Data Fusion - Equi Weight and Optimized

Proposed multi frequency EC Fusion model was implemented as discussed above and used as inverse problem solution to reconstruct the flaw profile of section C of aircraft fuselage. While results in terms of MSE have been illustrated, images of flaw profile (X-Ray image) and flaw profile re-constructed using proposed model applied on training data is shown in Figure-5-3 for comparison.

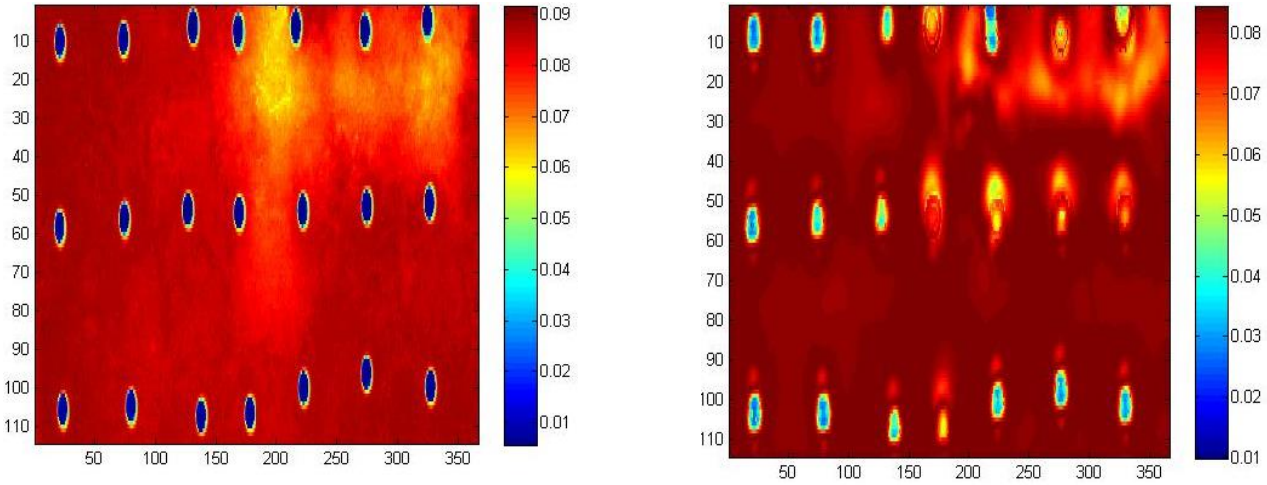

(a) Flaw Profile (X-Ray Image) (b) Reconstructed Image

Figure 5-3 (a) & (b) - The flaw profile (X-Ray image) and Re-constructed image of Sec C of Aircraft Fuse Loge

5.6 IMPLEMENTATION OF PROPOSED MULTIFREQUENCY EC FUSION MODEL ON TEST DATA

The optimized weighted polynomial model was applied on the EC data, scanned at multiple frequencies, of Section-D of the aircraft for validation of the approach. Results validated the model and the MSE values were lowest with the novel constrained weight optimized technique. Results in terms of MSE for equal and proposed constrained optimized fusion are placed at Table-5-4 and illustrated at Fig 5-5.

Table 5-4 RESULTS (MSE; 10^-5) – EQUAL AND OPTIMIZED FUSION MODELS

FIG 5-4 RESULTS (MSE; 10^-5) – EQUAL AND OPTIMIZED FUSION MODELS

Order	Data Fusion (Weights)	
	Equal (MSE; 10^{-5})	Optimized (MSE; 10^{-5})
2nd	8.69	8.37
3rd	8.69	8.56
4th	8.28	7.85
5th	8.43	7.99

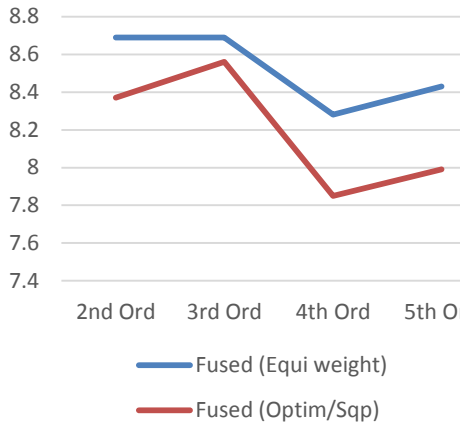

While results in terms of MSE have been tabulated, images of flaw profile (X-Ray image) of Section-D of fuselage (test/validation data mutually exclusive to training data) and flaw profile re-constructed using proposed Multi frequency EC fusion Model applied on test data is illustrated in Figure-5-5 for comparison.

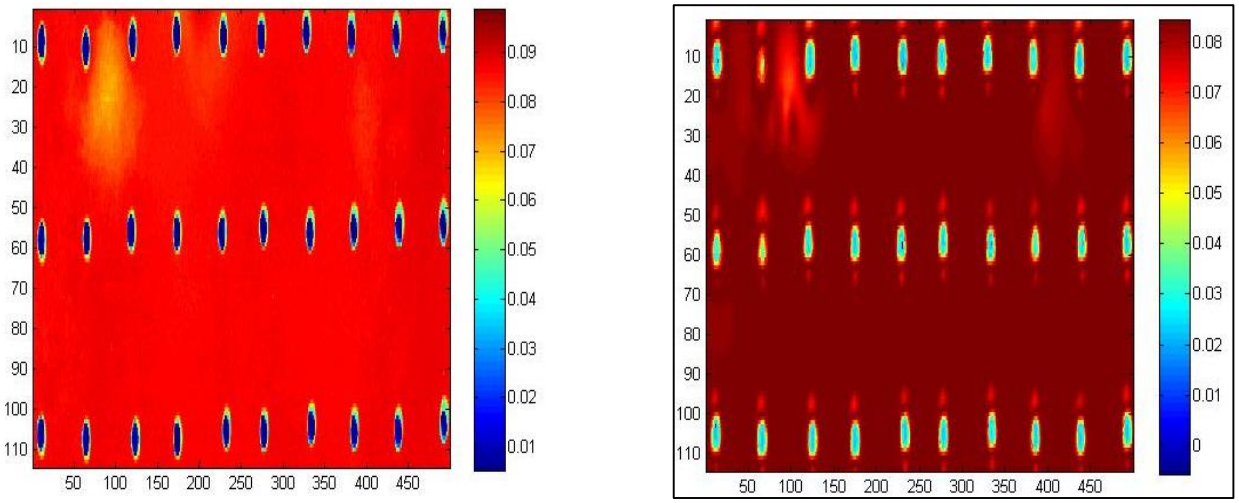

(a) Flaw Profile (X-Ray Image Section D) (b) Reconstructed Image Section D

Figure 5-5 (a) & (b) - The flaw profile (X-Ray image) and Re-constructed image of Sec D of Aircraft Fuse Loge

Chapter 6 Conclusion and Future Work

Actual X-Ray and Eddy Current Testing (ECT) data of aircraft fuselage was statistically analyzed. During general and then forward case analysis of the case study, it was observed that Eddy Currents Measurements are quite sensitive to changes in Truth Profile. For a change of flaw depth from 0.005 to 0.091 only, change in measurements from -7.9 to 6.2 approximately in magnitude was noted. Ill posedness of the problem was also observed owing to number of unique values of Truth profile (X-Ray data) and Multimode Measurement data.

Significance to consider neighbor flaw profile effect in EC measurement generation was also marked through percentage error (ratio of standard deviation and mean) study.

During analysis of neighboring flaw profile effect, it was found that low frequency of 8 kHz measurements were better re-constructed using max value of scan area whereas higher frequencies of 17 and 30 kHz were slightly better when re-constructed using Mean value of the scan area for forward measurement profile construction.

During Inverse problem flaw profiling through statistical technique, it has been observed that lower frequency of 8 kHz offered better results as compared to 17 & 30 kHz - the deduction is in line with skin depth effect according to which low frequency signal has ability to penetrate deeper in the specimen as discussed earlier. It was also

noted that higher polynomial models works better. Accordingly in the final model, 4th order Polynomial Model was selected and applied. Another important outcome of the work is the confirmation of the fact that the multi-mode (EC frequencies) carry complementary information. Optimized weighted Fusion of multi-mode EC signals offer more accuracy in the flaw profiling as compared to each of the individual mode results as well as Equi-Weight data fusion. The novel Model for inverse solution of ECT of aircraft fuselage is computationally efficient also and can be applied at run time for instant results. It was also noted that reconstructed technique was able to profile flaw variation as low as 0.0001 mm. Therefore, the novel constrained fusion based flaw profiling scheme using multiple frequency eddy current NDT of aero structures is an efficient technique which offer improved accuracy. Accordingly, same can be utilized by aerospace industry for instant flaw profiling in aircraft structure.

6.1 FUTURE WORK

As a future work, proposed model can be tested and new modelling can be allowed for materials other than aircraft structures. Similarly, fusion of multi-mode data using Constraint Optimization Technique can also be applied on other Non-Destructive Techniques such as Ultra-Sonic testing, Magnetic Flux Leakage (MFL) etc.

References

[1] G. C. Wilkinson, "Accident near Lusaka International Airport, Zamboa, on 14 may 1977," Aircraft Accident Report 9/78, Zambia, 1979.

[2] J. C. ,. a. I. S. R. Newman Jr, "Prediction of fatigue crack-growth patterns and lives in three-dimensional cracked bodies," in *ICF6*, New Delhi, India, 1984.2013.

[3] T. a. P. R. Khan, ""A recursive bayesian estimation method for solving electromagnetic nondestructive evaluation inverse problems."," *IEEE Transactions on Magnetics,* vol. 44, no. 7, pp. 1845-1855, 2008.

[4] D. S. F. J. P. K. K. H. a. T. K. Z. Liu, "Survey: State of the art in NDE data fusion techniques," *IEEE Transancations,* vol. 56, no. 6, pp. 2435-2451, Dec. 2007..

[5] B. M. B.-H. X. E. Gross, "NDT Data Fusion.," 1997.

[6] S. S. U. M. M. a. L. U. J. Yim, "“Optimum filter based techniques for data fusion,”," *in Review of Progress in QNDE, D. O. Thompson and D. E. Chimenti, Eds. New York: Plenum,* pp. 773-780, 1996.

[7] M. K. a. P. R. J. Dion, "“Multi-sensor data fusion for high-resolution material characterization,” in Proc. Rev. Prog. QNDE," in *in Proc. Rev. Prog. QNDE vol. 894, AIP Conference Proceedings, pp. 1189–1196.*, 2007.

[8] P. S. a. D. W. L. “. a. i. X. E. Gros, "“Theory and implementation of NDT data fusion,”," *Res. Nondestruct. Eval.,* vol. 6, no. 4, pp. 227-236.

[9] V. K. a. N. Francois, "“Use of data fusion methods to improve reliability of inspection: Synthesis of the work done in the frame of a European thematic network,”," in *in Proc. 8th ECNDT,* Barcelona, Spain,, Jun. 2002, vol. 8, no. 2, NDT. net.

[10] Z. L. a. K. H. X. E. Gros, "“Experimenting with pixel level NDT data fusion techniques,”," *IEEE Trans. Instrum. Meas,* vol. 49, no. 5, p. 1083–1090, Oct 2000.

[11] Y. W. S. a. S. S. Udpa, "“A new morphological algorithm for fusing ultrasonic and eddy current images,”," in *in Proc. IEEE Ultrason. Symp.,,* 1996, pp. 649–652..

[12] X. E. G. K. T. a. K. H. Z. Liu, "“3D visualization of ultrasonic inspection data by using AVS,”," in *in Proc. 5th Far-East Conf. Nondestruct. Test.,* Kenting, Taiwan, Nov. 1999, pp. 549–554.

[13] G. S. a. F. C.Morabito, "“NDT image fusion using eddy current and ultrasonic data,”," *COMPEL-Int. J. Comput. Math. Elect. Electron. Eng.,,* vol. 20, no. 3, pp. 857-868, 2001.

[14] D. S. Forsyth and J. P. Komorowski, "“The role of data fusion in NDE for aging aircraft,”," in *Proc. SPIE, vol. 3994, pp. 47–58*, 2000.

[15] S. S. U. L. U. T. X. a. W. L. K. Sun, "“Registration issues in the fusion of eddy current and ultrasonic NDE data using Q-transforms,”," in Review of Progress in QNDE, D. O. Thompson and D. E. Chimenti, Eds. New York Plenum, pp. 813–820., New York, 1996.

[16] T. K. a. P. Ramuhalli, "Sequential Monte Carlo methods for electromagnetic NDE inverse problems—Evaluation and comparison of measurement models," *IEEE,* vol. 45 No 3, no. Mar 2009, pp. 1566-1569, 2009.

[17] J. a. S. J. W. Nocedal, Numerical Optimization, Second Edition. Springer Series in Operations Research,, Springer Verlag, 2006.